Published in final edited form as:
ChemMedChem. 2012 January 2; 7(1): 49–52. doi:10.1002/cmdc.201100428.

Exhaustive Fluorine Scanning towards Potent p53-Mdm2 Antagonists

Yijun Huang[a,†], **Siglinde Wolf**[b,†], **David Koes**[c], **Grzegorz M. Popowicz**[b], **Carlos J. Camacho**[c], **Tad A. Holak**[b], and **Alexander Dömling**[a,*]

[a]Departments of Pharmaceutical Sciences and Chemistry, University of Pittsburgh, Pittsburgh, PA 15261, USA

[b]Max-Planck-Institute of Biochemistry, Am Klopferspitz 18, 82152 Martinsried, Germany

[c]Department of Computational and Systems Biology, University of Pittsburgh, Pittsburgh, PA 15261, USA

Keywords

multicomponent reaction; drug discovery; protein-protein interaction; p53-Mdm2; fluorine

The unmatched properties of the element fluorine are reflected in organic fluorine compounds. The richness of modern fluorine chemistry allows for the regioselective introduction of this element at virtually every position of a given molecule.[1, 2] Thus the introduction of fluorine has been especially valuable in the process of drug discovery to fine tune many different target and off-target related properties.[3–6] For example, fluorine has been used to increase the binding affinity of small molecules to its target,[7] to tune the pK_B and logD,[8] to improve target selectivity,[9] to improve oral absorption and exposure,[10] to prevent from metabolism[11] or to increase the antibacterial spectrum.[12] Not surprisingly, an estimated 20% of all pharmaceuticals contain fluorine.[4] Additionally, ^{18}F is often used as a positron emission tomography (PET) active element to perform time and space resolved distribution studies of drugs in animals and humans.[13, 14] Last but not least, ^{19}F is very useful in NMR of complex biological systems due to its high sensitivity and zero natural background.[15] Herein, we report the systematic F-scanning of a scaffold derived from the Ugi four-component reaction (Ugi-4CR) for the synthesis, optimization and biophysical characterization of potent p53-Mdm2 antagonists.

The protein-protein interaction (PPI) of the transcription factor p53 and its negative regulator Mdm2 has recently attracted great interest as a novel therapeutic concept to treat cancer.[16] The antagonistic compound RG7112 (a nutlin-3 derivative) is currently undergoing clinical trials, while several p53-Mdm2 antagonists are in preclinical development. Due to the wealth of structural information available for the p53-Mdm2 interaction,[17, 18] a pharmacophore-based virtual screening platform ANCHOR. QUERY was recently introduced for the rational design of small molecule antagonists.[19] Based on this approach we described a number of unprecedented multicomponent reaction scaffolds, which are able to efficiently disrupt the p53-Mdm2 interaction.[20, 21] A structurally characterized p53-Mdm2 antagonist **1** showed a nice alignment with the three-finger

Fax: (+)412-383-5298, asd30@pitt.edu.
To George Olah, a father of modern fluorine chemistry, for his 85th birthday.
†These authors contributed equally.

Supporting information for this article is available on the WWW under http://www.chemmedchem.org or from the author.

pharmacophore model for Mdm2 antagonists,[22] in which key moieties fit into the Trp23, Phe19 and Leu26 binding pockets.[23] Notably, the benzyl substituent of the small molecule involves an stacking interaction with the imidazole ring of His96 (Figure 1).[22] In an attempt to modulate the π-stacking interaction, all 19 isomers with different fluorine substitution pattern possible for the benzyl position were synthesized (Scheme 1). Fluorine substituted benzylamines **2b–t** were obtained from commercial sources or prepared from the corresponding benzylaldehydes by reductive amination.[24] MCR chemistry is efficient and straightforward, and the compounds **6a–t** were synthesized by the Ugi-4CR in good to excellent yields (supporting information [SI]). The ester group of **6a–t** was saponified to give the corresponding acid compounds **7a–t**, since 2-carboxylic acid of the indole ring is known to improve the binding affinity with Mdm2.[20] By the nature of the Ugi reaction, all products were formed as racemic mixtures and screened as such.

The binding constants (K_i) of the compounds **6** and **7** to Mdm2 were measured using our recently described fluorescence polarisation assay (Table 1, SI Table 1).[25] As a reference compound we used the well known nutlin-3a and the binding data well compare with previously publised results.[21] The acid compounds **7** show overall improved potency compared with the corresponding parent ethyl ester compounds **6**. Interestingly, the K_i values of compounds **7** with different fluorine substitution pattern varied by a factor of 44, between 5.7 μM and 130 nM. The best compound **7m** (K_i = 130 nM, molecular weight: 495 Da.) is amongst the most potent p53-Mdm2 antagonists known, which has comparable affinity to the reference compound nutlin-3a (K_i = 40 nM, molecular weight: 581.5 Da.). Compound **7m** exhibits a binding efficiency index (BEI) of 13.9, which indicates a better ligand efficiency than nutlin-3a (BEI = 12.7).[26] The aqueous solubility and calculated lipophilicity of **7m** is 0.85 mg/mL and cLogP = 3.69 (SI), which is superior compared to nutlin-3a (0.1 mg/mL, cLogP = 5.17).

In order to better understand the structural basis of the interaction, **7e** was co-crystallized with Mdm2 and the X-ray structure was resolved (Figure 2, SI Table 2). As expected, the small molecule binds into the p53 binding site of Mdm2. The 6-chloro-indol moiety aligns well with the anchor residue Trp23 of p53 and forms a hydrogen bond to Leu54. The 3,4-difluoro benzyl group mimics the Leu26 and the *tert*-butyl amide substituent derived from the isocyanide component is deeply buried in the Phe19 pocket. The formyl substituent points into the solvent space. Two amide oxygen atoms of **7e** and the residues in the receptor (His96 and Val93) form hydrogen bond bridges with surrounding water molecules (SI Figure 1). The overall interactions, however, are mostly governed by hydrophobic contacts involving the indol, 3,4-difluoro benzyl and *tert*-butyl substituent and its receptor amino acids (SI Figures 2–6). Clearly, the 3,4-difluoro benzyl group is nicely aligned parallel with the imidazole ring of His96 suggesting an attractive interaction. Short distances between the atoms of two aromatic rings are between 3.4–3.9 Å (SI Figure 4). Compared to other crystallographically characterized small molecule antagonists of the p53-Mdm2 interaction,[17, 18] the Leu26 binding site encloses the 3,4-difluoro benzyl group very tightly.

The enantiomers of **6e** and **6m** were efficiently separated by preparative supercritical fluid chromatography (SFC), and transformed to the corresponding enantiomers of **7e** and **7m**, respectively (SI). The enantiomer **(+)-7e** (Ki = 200 nM) is more potent than **(−)-7e** (Ki = 400 nM). Similarly, the enantiomer **(+)-7m** (Ki = 100 nM) is more potent than **(−)-7m** (Ki = 280 nM). Figure 3 shows a NMR heteronuclear single quantum coherence (HSQC) experiment for **(+)-7e** and Mdm2. A strong binding, with K_D of less than 1 μM, (and a slow chemical exchange) of **(+)-7e** to Mdm2 is indicated by signals doubling.[27]

A key property of the C-F bond is the reversed polarization as compared to the C-H bond. Thus, the pattern of fluorine substitutions on the benzene ring should be able to modulate the

aromatic interaction between the small molecule and its protein receptor.[28] We have investigated this effect using docking models derived from the co-crystal structure (Figure 2) by performing all possible fluorine substitution patterns in the benzyl group of compounds **7b–t** on a fixed receptor. All the refined docked small molecules show only minor differences relative to the co-crystal structure. The models reveal that the C-H to C-F substitution at the buried *ortho*-position leads to a highly repulsive dipole-dipole interaction (Figure 4). In fact, the straightforward change in Coulomb energy due to the charge swap indicated in Fig. 4 is about 4 kcal/mol. Not surprisingly, the fluorine in the buried *ortho*-position does not rank well either in our models or in the experiments. Note that at least for the subset of compounds with symmetric fluorine patterns there is no ambiguity on the position of the fluorines in the docked models based on the cocrystal structure.

Given the strong electrostatic coupling between the two rings, we expected the inter-molecular component of the electrostatic free energy to be the main determinant of binding affinity. Indeed, as shown in Figure 5, the correlation coefficient between the computed change in electrostatics and the experimentally determined affinity (pKi) yielded a strikingly accurate R = 0.96 for compounds with symmetric fluorine substitutions. The analysis correctly ranks compounds with the best and worst Ki values among the benzyl rings with symmetric F-pattern. By itself, this result is quite impressive since most physically based scoring functions do not recapitulate thermodynamic data.[29] The correlation of electrostatics with pKi for the full set of compounds, including those with fluorine substitutions that form asymmetric patterns, sharply drops to R = 0.58. An even lower correlation (R = 0.22) is obtained using the full binding affinities calculated by the software OpenEye Szybki, further emphasizing the key role of electrostatics in capturing changes in Ki for the different ligands. Refining the ligand protonation states by considering pKa and tautomer enumeration with the AM1-BCC charge model of OpenEye QuacPac version 1.3.1 do not change results.[30] The conspicuous over-prediction of the electrostatic component of the binding free energy for asymmetric compounds is likely to reflect the specificities of the internal energies for each rotamer of the benzyl ring. This effect is offset for symmetric compounds, but it should significantly affect the free energy of the unbound asymmetric ligands in ways that are ignored by the fixed ligand structures imposed by the Poisson-Boltzmann calculations.

In summary, we have efficiently synthesized 20 derivatives of p53-Mdm2 antagonist **1** via a one-pot Ugi-4CR including all possible fluorine substitutions on the benzyl group in order to optimize aromatic interactions. A co-crystal structure of **(*S*)-7e** with Mdm2 reveals the structural basis of the potent interaction. The introduction of fluorine substitutions on the benzyl group can considerably improve the potency of p53-Mdm2 antagonists, due to the electrostatic interaction between the small molecules and the receptor. Although limited in scope, the computational analysis of docked configurations that are presumed to bind using the same binding mode shows that the electrostatics of unique rigid structures can be reasonably be accounted for by current methods, whereas assessing the free energy of an unbound state with a variety of hard to evaluate internal states is quite detrimental to empirical estimates of the free energy. Our findings underscore the in principal known but often surprising effects, fluorine can exert on the biological activity of small molecules. Our findings may also lead medicinal chemists successful in modulating molecular interactions with other types of targets.

Supplementary Material

Refer to Web version on PubMed Central for supplementary material.

Acknowledgments

This work was supported by the NIH grants 1R21GM087617-01, 1P41GM094055-01, 1R01GM097082-01 and Qatar Foundation NPRP 4-319-3-097 (to AD), Deutsche Krebshilfe, Grant 108354 (to TH), and is part of a NCI-NExT program.

References

1. Olah, GA.; Chambers, RD.; Surya Prakash, GK., editors. Synthetic Fluorine Chemistry. New York: Wiely; 1992.
2. Shimizu M, Hiyama T. Angew. Chem. Int. Ed. 2005; 44:214–231.
3. (a) Müller K, Faeh C, Diederich F. Science. 2007; 317:1881–1886. [PubMed: 17901324] (b) Salonen LM, Ellermann M, Diederich F. Angew. Chem. Int. Ed. 2011; 50:4808–4842.
4. Böhm H-J, Banner D, Bendels S, Kansy M, Kuhn B, Müller K, Obst-Sander U, Stahl M. Chem Bio Chem. 2004; 5:637–643.
5. Hagmann WK. J. Med. Chem. 2008; 51:4359–4369. [PubMed: 18570365]
6. Purser S, Moore PR, Swallow S, Gouverneur V. Chem. Soc. Rev. 2008; 37:320–330. [PubMed: 18197348]
7. Backes BJ, Longenecker K, Hamilton GL, Stewart K, Lai C, Kopecka H, von Geldern TW, Madar DJ, Pei Z, Lubben TH, Zinker BA, Tian Z, Ballaron SJ, Stashko MA, Mika AK, Beno DWA, Kempf-Grote AJ, Black-Schaefer C, Sham HL, Trevillyan JM. Bioorg. Med. Chem. Lett. 2007; 17:2005–2012. [PubMed: 17276063]
8. Morgenthaler M, Schweizer E, Hoffmann-Röder A, Benini F, Martin RE, Jaeschke G, Wagner B, Fischer H, Bendels S, Zimmerli D, Schneider J, Diederich F, Kansy M, Müller K. Chem Med Chem. 2007; 2:1100–1115. [PubMed: 17530727]
9. Su H, Xie Y, Liu W-B, You S-L. Bioorg. Med. Chem. Lett. 2011; 21:3578–3582. [PubMed: 21602044]
10. Kerekes AD, Esposite SJ, Doll RJ, Tagat JR, Yu T, Xiao Y, Zhang Y, Prelusky DB, Tevar S, Gray K, Terracina GA, Lee S, Jones J, Liu M, Basso AD, Smith EB. J. Med. Chem. 2011; 54:201–210. [PubMed: 21128646]
11. Park BK, Kitteringham NR, O'Neill PM. Ann. Rev. Pharm. Tox. 2001; 41:443–470.
12. Percival A. J. Antimicrob. Chemother. 1991; 28:1–8. [PubMed: 1787126]
13. Le Bars D. J. Fluorine Chem. 2006; 127:1488–1493.
14. Cai L, Lu S, Pike VW. Eur. J. Org. Chem. 2008; 2008:2853–2873.
15. Yanamala N, Dutta A, Beck B, Van Fleet B, Hay K, Yazbak A, Ishima R, Dömling A, Klein-Seetharaman J. Chem. Biol. Drug Des. 2010; 75:237–256. [PubMed: 20331645]
16. Cheok CF, Verma CS, Baselga J, Lane DP. Nat. Rev. Clin. Oncol. 2011; 8:25–37. [PubMed: 20975744]
17. Khoury K, Popowicz GM, Holak TA, Dömling A. Med Chem Comm. 2011; 2:246–260.
18. Popowicz GM, Dömling A, Holak TA. Angew. Chem. Int. Ed. 2011; 50:2680–2688.
19. Koes D, Khoury K, Huang Y, Wang W, Bista M, Popowicz GM, Wolf S, Holak TA, Dömling A, Camacho CJ. PLoS Compu. Biol. in press.
20. a) Czarna A, Beck B, Srivastava S, Popowicz GM, Wolf S, Huang Y, Bista M, Holak TA, Dömling A. Angew. Chem. Int. Ed. 2010; 49:5352–5356.b) Huang Y, Wolf S, Bista M, Meireles L, Camacho C, Holak TA, Dömling A. Chem. Biol. Drug Des. 2010; 76:116–129. [PubMed: 20492448] c) Srivastava S, Beck B, Wang W, Czarna A, Holak TA, Dömling A. J. Comb. Chem. 2009; 11:631–639. [PubMed: 19548636]
21. Popowicz GM, Czarna A, Wolf S, Wang K, Wang W, Dömling A, Holak TA. Cell Cycle. 2010; 9:1104–1111. [PubMed: 20237429]
22. Wolf S, Huang Y, Popowicz GM, Goda S, Holak TA, Dömling A. J. Am. Chem. Soc. in revision.
23. Dömling A. Curr. Opin. Chem. Biol. 2008; 12:281–291. [PubMed: 18501203]
24. Ono T, Kukhar VP, Soloshonok VA. J. Org. Chem. 1996; 61:6563–6569. [PubMed: 11667521]
25. Popowicz G, Czarna A, Holak T. Cell Cycle. 2008; 7:2441–2443. [PubMed: 18677113]

26. Abad-Zapatero C, Metz JT. Drug Discov. Today. 2005; 10:464–469. [PubMed: 15809192]
27. a) Wüthrich, K. NMR of Proteins and Nucleic Acids. New York: Wiley; 1986. b) Rehm T, Huber R, Holak TA. Structure. 2002; 10:1613–1618. [PubMed: 12467568]
28. a) Kim CY, Chang JS, Doyon JB, Baird TT, Fierke CA, Jain A, Christianson DW. J. Am. Chem. Soc. 2000; 122:12125–12130.b) Kim CY, Chandra PP, Jain A, Christianson DW. J. Am. Chem. Soc. 2001; 123:9620–9627. [PubMed: 11572683]
29. Warren GL, Andrews CW, Capelli AM, Clarke B, LaLonde J, Lambert MH, Lindvall M, Nevins N, Semus SF, Senger S, Tedesco G, Wall ID, Woolven JM, Peishoff CE, Head MS. J. Med. Chem. 2006; 49:5912–5931. [PubMed: 17004707]
30. Wlodek S, Skillman AG, Nicholls AJ. Chem. Theory Comput. 2010; 6:2140–2152.

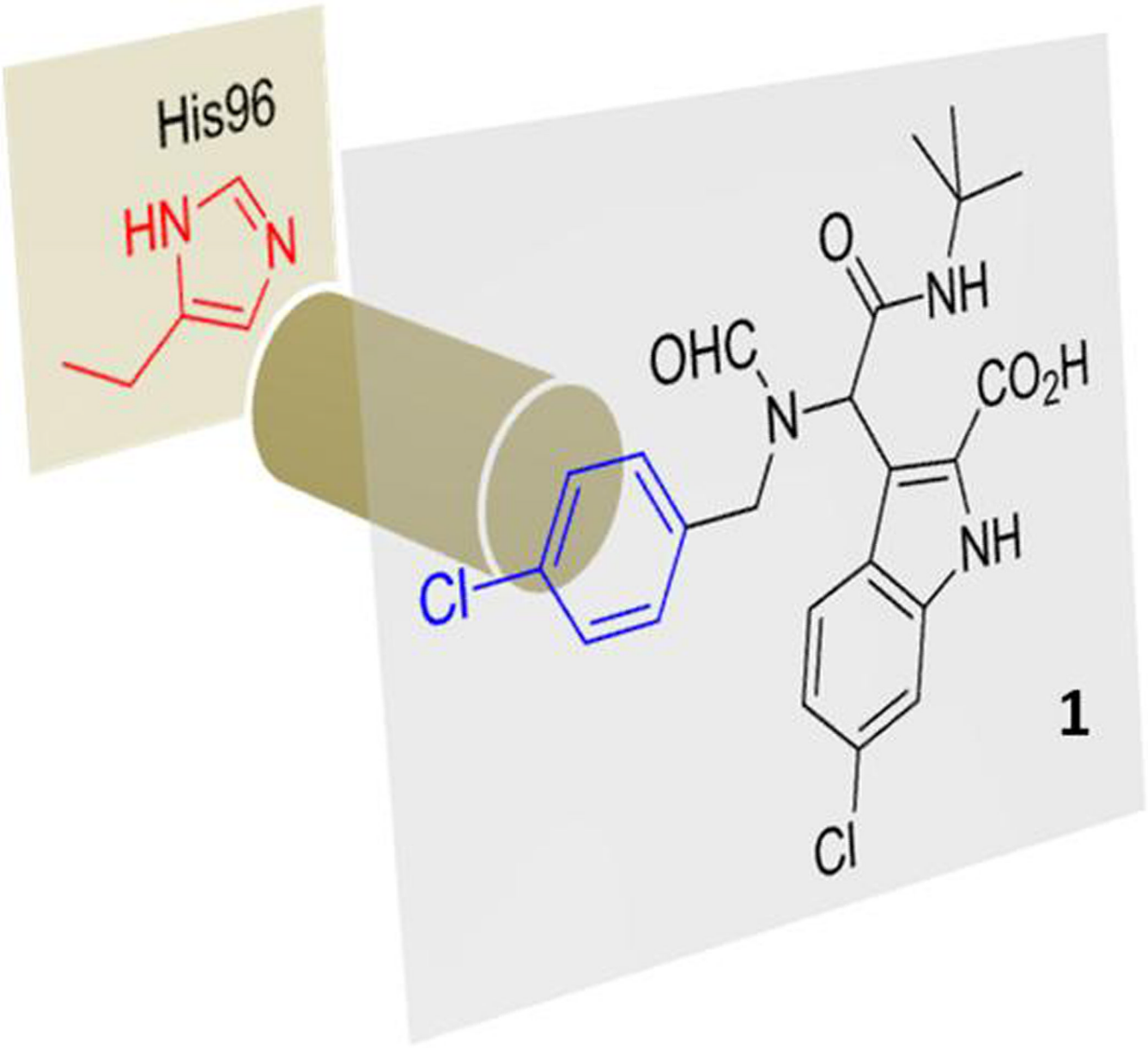

Figure 1.

A co-crystal structure of p53-Mdm2 antagonist **1** reveals a parallel alignment between the benzyl group of the Ugi scaffold and the imidazole ring of His96 (Mdm2), which seems suitable for optimization of the π-π interaction.[22]

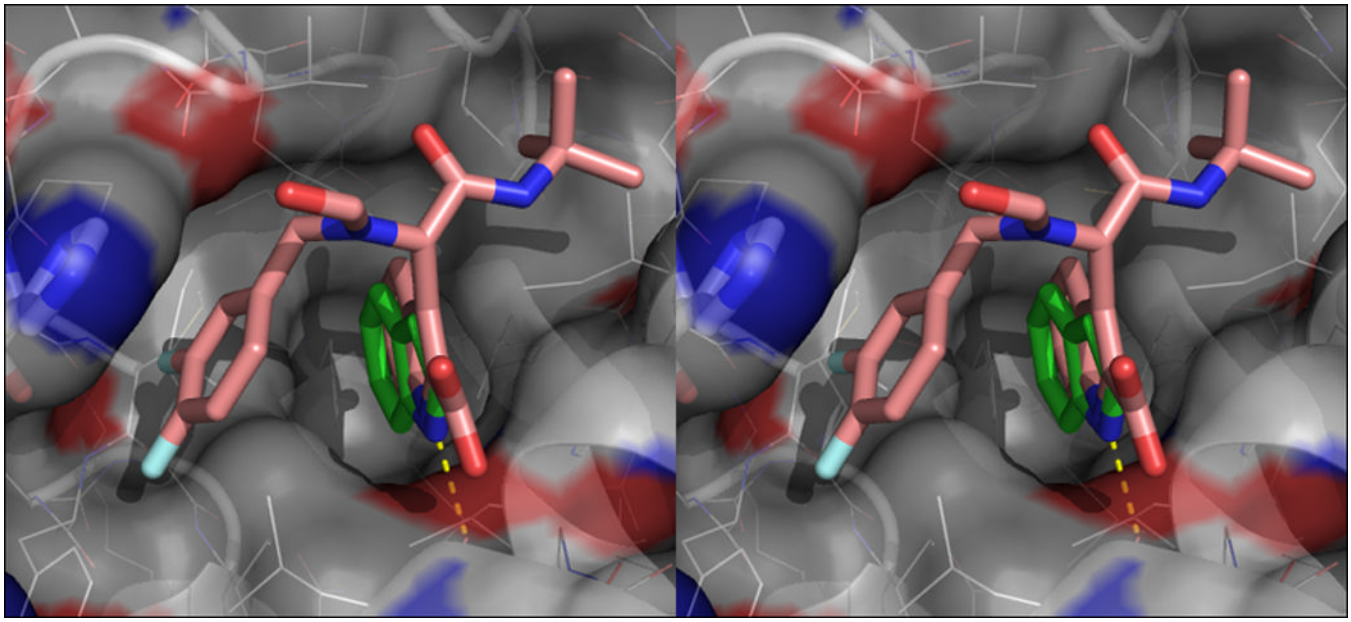

Figure 2.
Stereo picture of compound **(*S*)-7e** (pink sticks) in Mdm2 (surface with cartoon secondary structure and lines). His96, forming a π-stacking interaction with the 3,4-difluoro benzyl group of **(*S*)-7e** is highlighted as blue sticks. The indol fragment of **(*S*)-7e** aligns well with the anchor fragment Trp23 of p53 (green sticks, PDB ID: 1YCR; RMSD = 0.701 Å). The indol NH of **(*S*)-7e** also forms the characteristic conserved hydrogen bond with the carbonyl group of Leu54 (yellow dotted line).

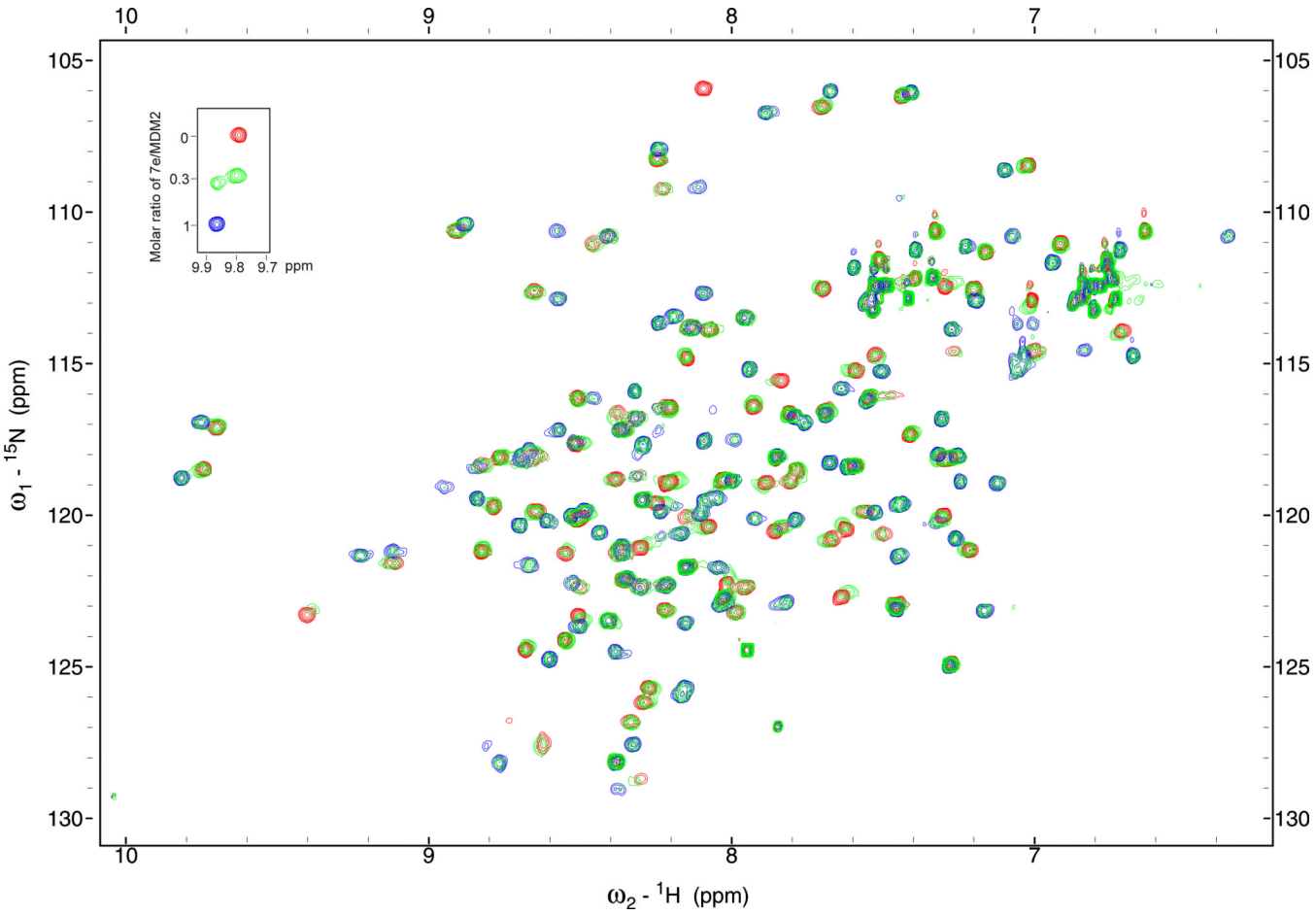

Figure 3.

Superposition of NMR HSQC spectra of ^{15}N-labeled Mdm2 titrated against **(+)-7e**. The spectrum of free Mdm2 is shown in red. The spectrum of **(+)-7e**-Mdm2 (intermediate ratio, 3:10, respectively) is shown in green, and the spectrum of **(+)-7e**-Mdm2 (final ratio, 1:1) is shown in blue.

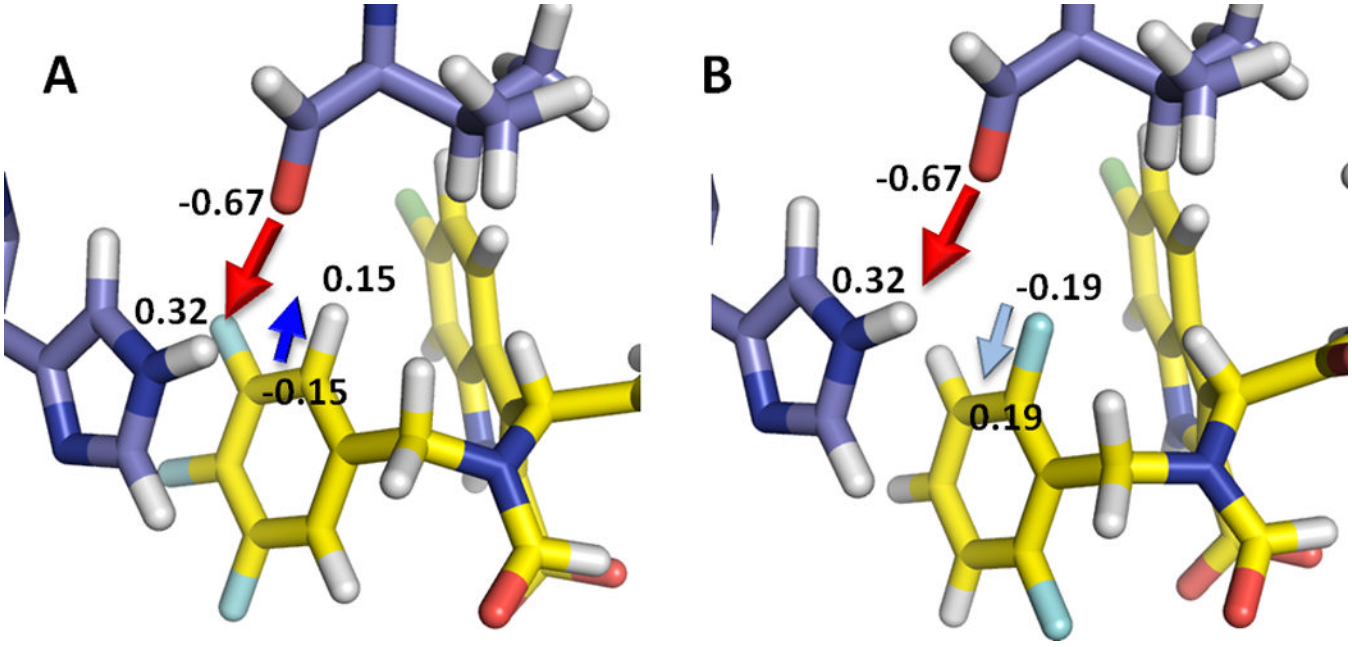

Figure 4.

Dipole reversal by fluorine is the main determinant of binding affinity. Docking models (yellow sticks) of (A) compound **(*S*)-7m** and (B) compound **(*S*)-7j** are minimized structures of the superposition of the small molecules onto the ligand of the co-crystal shown in Fig. 2 with a fixed receptor. Arrows depict the dipole-dipole interaction between the His96.ε-Val93.O hydrogen bond (blue sticks, red arrow) and the (A) C-H (blue arrow) and (B) C-F (cyan arrow) dipoles that are attractive and repulsive, respectively. Also indicated are the MMFF (Merck Molecular Force Field) partial charges.

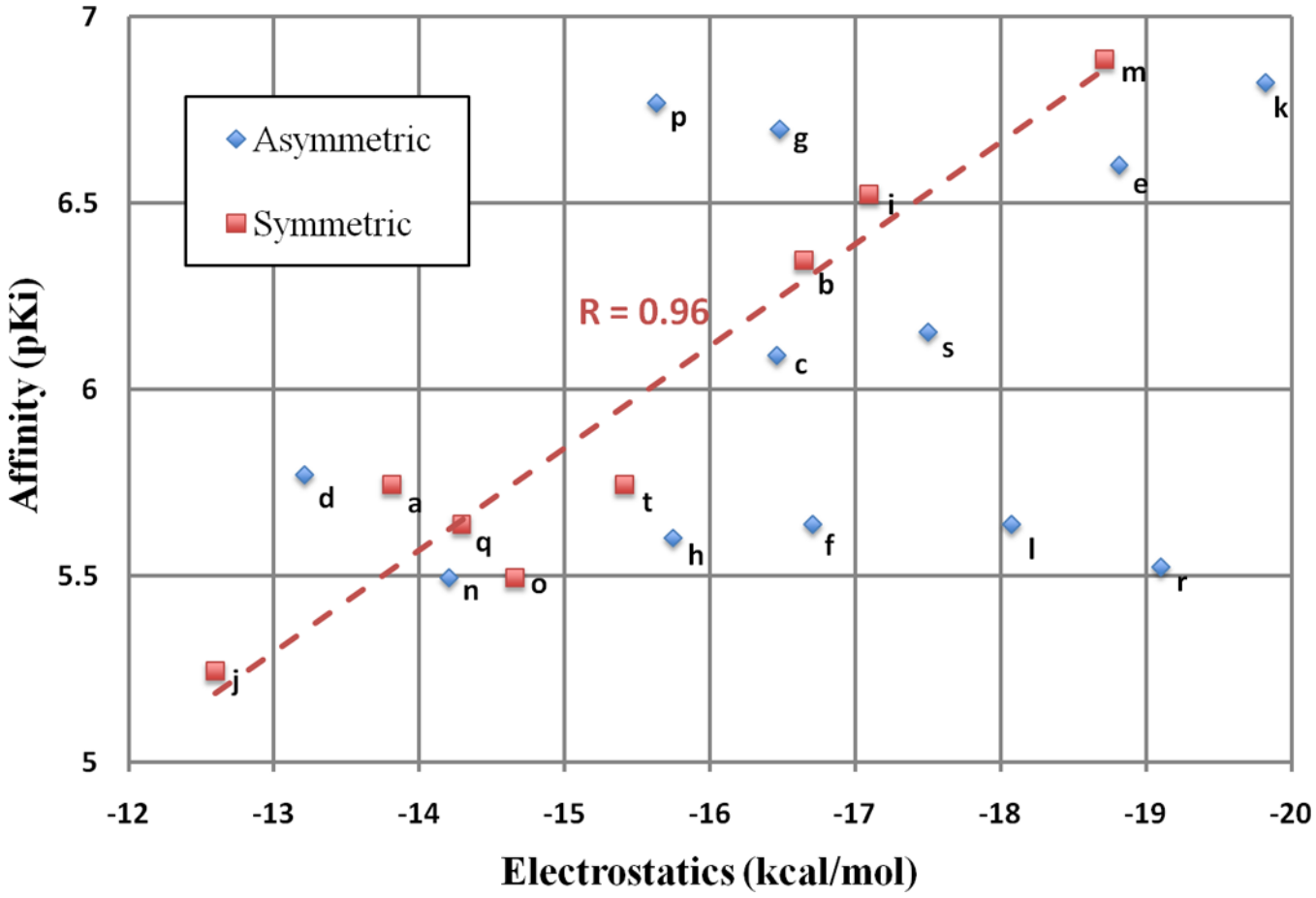

Figure 5.

Correlation between the calculated change in electrostatics and binding affinity (pKi) for compounds (*S*)-7. Electrostatic calculations were performed using OpenEye Szybki 1.3.1 with a Poisson-Boltzmann solvation model and MMFF partial charges. Compounds with a symmetric arrangement of fluorine atoms in the benzyl group correlate closely (R = 0.96) to the calculated electrostatics. The remaining asymmetric compounds are more difficult to characterize and reduce the overall correlation (R = 0.58). Following Table 1, letters indicate the fluorine substitution pattern in the phenyl ring.

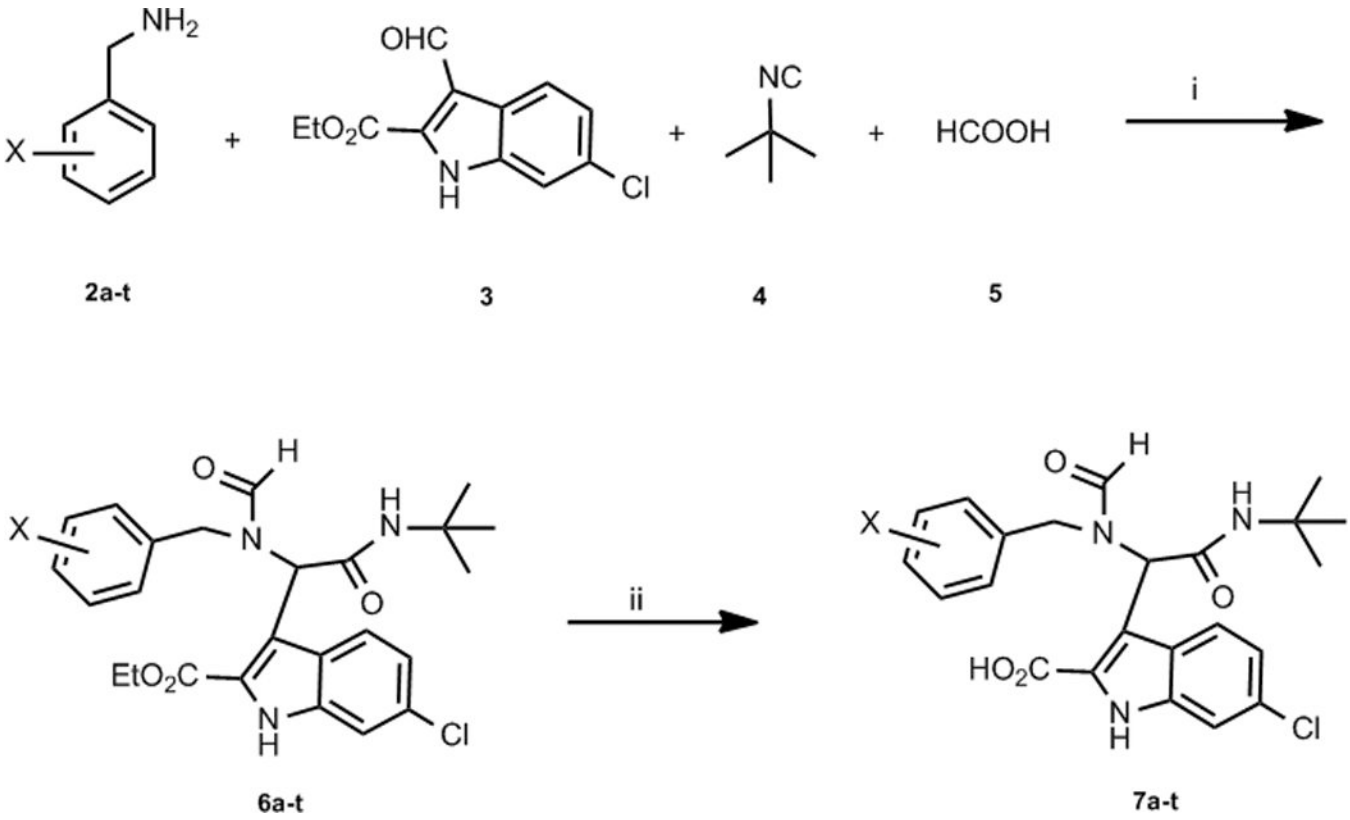

Scheme 1.

Synthesis of p53-Mdm2 antagonists using the Ugi-4CR followed by saponification. Conditions: (i) MeOH, r.t.; (ii) LiOH, EtOH/H_2O (1:1), r.t..

Table 1

Inhibition constants [μM] of compounds **6** and **7**.

No.	X	K_i (6) [a]	K_i (7) [a]	cLogP (7) [b]
a	H	1.5	1.8	3.26
b	4-F	2.2	0.45	
c	3-F	1.3	0.81	3.40
d	2-F	3	1.7	
e	3,4-F	0.5	0.25	
f	2,4-F	6	2.3	
g	2,3-F	3	0.2	3.54
h	2,5-F	10	2.5	
i	3,5-F	2.4	0.3	
j	2,6-F	4.5	5.7	
k	2,3,4-F	2.1	0.15	
l	2,4,5-F	5	2.3	
m	3,4,5-F	0.4	0.13	3.69
n	2,3,6-F	4.3	3.2	
o	2,4,6-F	6.8	3.2	
p	2,3,5-F	2.5	0.17	
q	2,3,5,6-F	6.7	3	
r	2,3,4,6-F	5.8	3	3.83
s	2,3,4,5-F	7	0.7	
t	2,3,4,5,6-F	5.8	1.8	3.97
Nutlin-3a			0.04	5.17

*[a]*Measured by fluorescent polarization assay.

*[b]*Calculated using Instant JChem 2.5.3 from ChemAxon.